

Article

Solubility of Camphene and Caryophyllene Oxide in Subcritical and Supercritical Carbon Dioxide

Hooi S. Yeoh^{1,a}, Thomas S. Y. Choong¹, Noranizan Mohd Adzahan²,
Rusly Abdul Rahman², and Gun H. Chong^{2,b,*}

¹ Department of Chemical and Environmental, Faculty of Engineering, Universiti Putra Malaysia, 43400 UPM, Serdang, Selangor, Malaysia

² Department of Food Technology, Faculty of Food Science and Technology, Universiti Putra Malaysia, 43400 UPM, Serdang, Selangor, Malaysia

E-mail: ^ahsimvalley@yahoo.com, ^bgunhean@upm.edu.my (Corresponding author)

Abstract. The solubility of camphene and caryophyllene oxide in subcritical and supercritical carbon dioxide were determined using dynamic off-line analysis method. Under subcritical condition, solubility of camphene and caryophyllene oxide were $(1.738 \text{ to } 18.118) \cdot 10^{-3}$ and $(1.84 \text{ to } 7.872) \cdot 10^{-3}$ respectively at 298.15 K with pressure varied from 50 to 70 bar. At 302.15 K and under same pressure variation, solubility of camphene and caryophyllene oxide were $(1.918 \text{ to } 18.76) \cdot 10^{-3}$ and $(14 \text{ to } 25.624) \cdot 10^{-3}$ respectively. Under supercritical condition, experiments were run from 80 bar to 250 bar. Solubility of camphene was ranged from $(54.024 \text{ to } 151.67) \cdot 10^{-3}$ at 308.15K and $(17.552 \text{ to } 65.487) \cdot 10^{-3}$ at 313.15 K; while solubility of caryophyllene oxide was ranged from $(24.9 \text{ to } 299.94) \cdot 10^{-3}$ at 308.15 K and $(2.542 \text{ to } 102.359) \cdot 10^{-3}$ at 318.15 K. These solubility data was correlated with three semi-empirical models which were Bartle, Chrastil and Mendez-Santiago-Teja model. Of these three models, Mendez-Santiago-Teja model showed excellent fitting with average absolute relative deviation kept below 2%.

Keywords: Solubility, supercritical, subcritical, carbon dioxide, camphene, caryophyllene oxide.

ENGINEERING JOURNAL Volume 19 Issue 4

Received 8 September 2014

Accepted 7 January 2015

Published 31 July 2015

Online at <http://www.engj.org/>

DOI:10.4186/ej.2015.19.4.93

1. Introduction

Supercritical and subcritical fluid technology has received much attention lately because it is environmental friendly, less contamination on end product, energy saving and controllable [1–3]. Changes of thermodynamic property like density with little variation of temperature and pressure are intense in subcritical condition. Therefore, it is interesting to know the solubility behavior of solute in subcritical fluid.

A substance has three common distinct phases that exist with different thermodynamic conditions, namely solid, liquid and gas. These three phases have clear phase boundary and at the condition of phase boundary line, multiphase of matter occurs and stay equilibrium with each other. At the triple point, the three equilibrium lines intersect and solid, liquid and gas can coexist and stay in stable equilibrium [4]. Besides the three phases that widely known, there are actually 2 more phases which are not commonly mentioned, the subcritical phase and supercritical phase. As critical pressure and temperature of carbon dioxide is 7.28 MPa and 304.1 K, supercritical carbon dioxide exists at condition beyond these values. Subcritical phase is a condition that its pressure and temperature near the critical value, yet still slightly below it [5]. Subcritical fluid is liquid under critical pressure but its temperature is between the boiling point and critical point. It is also known as superheated liquid or pressurized hot liquid. This superheating phenomenon is also referred as boiling retardation or boiling delay, where liquid is heated to a temperature higher than its boiling point without boiling. There is no clear boundary of subcritical carbon dioxide as documented in literature, thus, in this study, the range of subcritical carbon dioxide has been determined from 50 – 70 bar, with temperature at 298.15 K and 303.15K due to constraints of experimental setup and material physical property.

In this work, solubility behavior study in subcritical carbon dioxide was covered to have a general comparison between supercritical and subcritical in the aspect of solubility trend. Carbon dioxide was used as the solvent because it is inexpensive, easily obtained in high purity, chemically stable, nontoxic, safe, mild, does not damage solute and matrix of products [6], and harmless to environment [7]. Camphene and caryophyllene oxide were selected as compound to study because their solubility data in supercritical carbon dioxide is still unavailable.

Caryophyllene oxide can be found abundantly in black pepper (*Piper nigrum* L.) which is a compound that contributes to spiciness. It is used as betel leaf substitute which contains arecoline that will cause parasympathetic effect such as pupillary and bronchial constriction [8]. It also has fumigant and insecticidal properties which can use in pest and weed control [9]. Additionally, it has antispasmodic agents that are used to treat rheumatism and painful spleen and was reported to possess analgesic, antipyretic, antiseptic and abortifacient properties [10]. Camphene is originated from peacock ginger (*Kaempferia rotunda*) which has been used to make ointments to treat scabies and itch. It can be used to synthesize camphor and insecticide.

Both of these compounds can be made into essential oils and they have antioxidant effect which can help reduce the toxin effects in the body and promote good health [11, 12]. Caryophyllene oxide and camphene are also commonly used as flavor and fragrance agent. Both compounds have been disclosed for their biological benefits of anti-cancer, anti-inflammatory, anti-fungal, anti-gastric ulcer and are also used in treatment for cardiovascular disease and as adjuvant [13]. The anti-fungal property can be used to preserve food, drug and cosmetic [14].

Supercritical carbon dioxide technology is favored because it is green [15] and suitable for food and pharmaceutical grade products because it leaves no solvent residue in the extract [16]. Solubility data of these compounds in supercritical carbon dioxide is useful in extraction, purification, particle formation, and separation process. Nowadays, solubility data of many active compounds from herbs have been presented [15, 17–23]. However, no literature of solubility data in supercritical carbon dioxide is available for camphene and caryophyllene oxide where in near future the importance of solubility data for these components will be increased due to their usage and benefits of supercritical fluid technology. With the solubility data, their medicinal properties can also be further discovered and exalted. Objectives of this work are to investigate the temperature and pressure effect on camphene and caryophyllene oxide solubility as well as to identify suitable mathematical model to correlate these data.

2. Experimental Section

Camphene and caryophyllene oxide with purity 95% from Sigma Aldrich (United States) was used. The solvent used was purified carbon dioxide liquefied under pressure from MOX-Linde Gas (Malaysia). Dynamic method coupled with gravimetrically analysis was opted because it is cheaper, not subject to leakage from valve and fittings, easier and faster operation, easy assembly of apparatus, and large amount of equilibrium data can be produced easily. Aside to this dynamic method, a more thorough review on the types of solubility measurement method has been discussed in previously published paper [24]. The rig consisted of two main parts, which are equilibrium unit and quantification unit. The front part which is the equilibrium unit mainly consisted of positive displacement pump, oven, preheating coil, and equilibrium cell. The latter part which is the quantification unit consisted of back pressure regulator, solute trap and gas meter. The experimental apparatus was prior validated with naphthalene solubility data from McHugh and Paulitis [25] to justify its accuracy and workability. The schematic diagram of experimental apparatus was shown in Figure 1.

Excess amount of solute was filled into the equilibrium cell to ensure that the exit stream of carbon dioxide was saturated with solute. Glass beads were added together to increase mass transfer rate and improve the equilibrium condition between solute and the supercritical fluid. Glass wool was plugged at top and bottom of equilibrium cell used to prevent solute escape from the equilibrium cell at high flow rates and at high pressure when density of supercritical carbon dioxide is higher than solute. Carbon dioxide from the supply tank is drawn into positive displacement pump (model SFC-24, Chrom Tech, United States) and pressure was regulated through back pressure regulator (series 26-1700, Tescom, United States). Temperature of the system was controlled by an oven (model UFE 600, Memmert, Germany) with a PID microprocessor controller and integrated auto-diagnostic system. A 3 m long preheating coil was installed to ensure the carbon dioxide solvent reached system temperature before contacted with solute. The equilibrium cell is designed as long and narrow cylinder with its both end covered with stainless steel frits. Length of the equilibrium cell is 20 cm and its diameter is 1 cm to allow it to be fitted in the oven. In the equilibrium cell, a thermocouple (model TR-40, WIKA, United States) was inserted to ensure the temperature inside the equilibrium cell was maintained at the desire value with display (model SR1, Shimaden, Japan). Pressure transmitter (model S-10, WIKA, United States) was installed to the equilibrium cell and displayed pressure of system through digital indicator (model DI15, WIKA, United States). Flow rate of carbon dioxide was validated with literature [25] and determined at 4 ml/min. After back pressure regulator, solute that solubilized in carbon dioxide stream was precipitated in solute trap, leaving the lean carbon dioxide to dry gas meter to record totalized mass flow rate. The amount of trapped solute was measured gravimetrically and dry gas meter (model TopTrak 822, Sierra, United States) was specially calibrated to measure carbon dioxide flow rate. Duplicate run of experiment was conducted and a final mean value was obtained. The solubility of solid solute in subcritical and supercritical carbon dioxide was determined by the following equation:

$$y_2 = \frac{W_2 / M_2}{(W_1 / M_1) + (W_2 / M_2)} \quad (1)$$

where y_2 is the solubility of the solute in carbon dioxide, W_2 is the mass of trapped solute, M_2 is the molecular weight of solute, W_1 is the mass of carbon dioxide, and M_1 is the molecular weight of carbon dioxide. Experiments were run for all solutes in the conditions stated in Table 1.

3. Result and Discussion

In the experiment of supercritical condition, both camphene and caryophyllene oxide melted at temperature lower than their melting point, which is 321.15 K (48 °C) for camphene and 333.15 K (60 °C) for caryophyllene oxide; and this could due to complex behavior change in supercritical condition [6, 23, 26, 27], which makes the solubility behavior study limited by temperature constraint. Figs. 2 and 3 showed phase behavior of camphene and caryophyllene oxide in subcritical condition while Figs. 4 and 5 showed phase behavior of camphene and caryophyllene oxide in supercritical condition respectively. The solubility data produced was tabulated in Table 2 and 3.

From Figs. 2 and 3, solubility of solute increased significantly with minor increase of pressure and temperature because density of carbon dioxide was extremely sensitive in subcritical region [28]. Both

solutes have higher solubility at higher temperature as this is a typical condition in dissolving reaction where increase of temperature gives more heat to break apart the solute and result high solubility of solute in solvent. When heat is received to break intermolecular bonding, physical state of solid begins to change which causes sublimation pressure of solid increases [29]. This increment of sublimation pressure favours the exothermic process and allows more solute to solubilize in carbon dioxide as this decreases the solute-solute interaction [30]. Although solvent power of carbon dioxide decreased at higher temperature, solubility of solute was still noted higher because sublimation pressure effect of solute which was a dominant effect increased with temperature and enhances the solubilization [18, 31]. In subcritical region, solubility increased considerably with slight increment of pressure and temperature, which exhibited exponential pattern when graph of solubility against pressure was plotted. This could be because carbon dioxide was oscillating between gas and liquid phase with slight change of environment condition. Density of carbon dioxide could increase greatly when gas phase turned to liquid phase, which the solvating power could increase significantly [32]. Thus, solvating power of subcritical carbon dioxide could not be controlled so well by regulating pressure as supercritical carbon dioxide [33]. As compared of Fig. 3 to Fig. 2, the scale interval of x-axis for Fig. 3 is inconsistent with Fig. 2. This is mainly because there are limited ranges of pressure and temperature can be studied in the subcritical condition for caryophyllene oxide due to extreme changes in solubility value with slight variation of system condition and system setup constraints. As pressure goes below 60 bar, no caryophyllene oxide is detected to solubilize in carbon dioxide, which is the main factor that causes only three data available. In addition to this, the system setup has constraint that back pressure regulator is unable to perform minute adjustment of pressure. However, this study still covered the subcritical zone of carbon dioxide with caryophyllene oxide solubility study.

From Fig. 4, at supercritical condition, solubility behavior of camphene is less sensitive to increasing pressure compared to subcritical condition while from Fig. 5, solubility of caryophyllene oxide still exhibited exponential pattern where solubility increased dramatically with pressure. At supercritical region, higher solubility was noted at lower temperature [34]. This is the behavior of retrograde where density of carbon dioxide dominates over sublimation pressure of caryophyllene oxide [18]. Retrograde is an unusual condition that solubility of solute decreases when temperature increases in a certain pressure range while at other pressure range, solubility increases with increasing temperature [28]. This condition makes solubility behavior of solute an unpredictable trend towards changing of temperature where temperature might increase, decrease or have no effect on solubility of solute depending on pressure. Within the retrograde vaporization region, density effect of carbon dioxide dominates over sublimation pressure of solute and cause higher solubility at lower temperature. However, solubility is still commonly increases with increasing pressure because density of carbon dioxide is increased which reduces intermolecular spaces between solvent and increases interaction between solute and solvent [35]. Solvating power has direct relation with density, so when density increases, more solid can be solubilized. Thus, increases of pressure can increase the solvating power of supercritical carbon dioxide [36].

4. Mathematical Modelling

There are many types of mathematical models can be used to correlate the solubility data as described in our previous published paper [24]. Mathematical correlation models are useful because they help to determine solubility of solute at every different point of working condition, which is infeasible to determine through experimental approach. In our current study, experimental data was correlated using Bartle model [37], Chrastil model [38] and Mendez-Santiago-Teja (MST) model [39], as shown in Table 4. Semi-empirical models are used to describe the general phase behavior at thermodynamic conditions other than experimental because they have less computationally complexity and difficulties in evaluating unknown parameters. These three semi-empirical models used correlate solubility data to density of carbon dioxide. Density value of supercritical carbon dioxide was obtained from Gupta and Shim [40] works, which employed Span and Wagner (1996) equation of state for the calculation of PVT properties.

In the work of finding appropriate model to fit the experimental solubility data, percentage of average absolute relative deviation (AARD) was calculated to check conformity of model to experimental data, which is as shown:

$$\text{AARD}(\%) = \frac{1}{N} \sum \frac{|Y^{\text{model}} - Y^{\text{exp}}|}{Y^{\text{exp}}} \times 100 \quad (2)$$

where N is the total number of data, Y^{model} is the y-axis value predicted from model, Y^{exp} is the y-axis value calculated from experimental data.

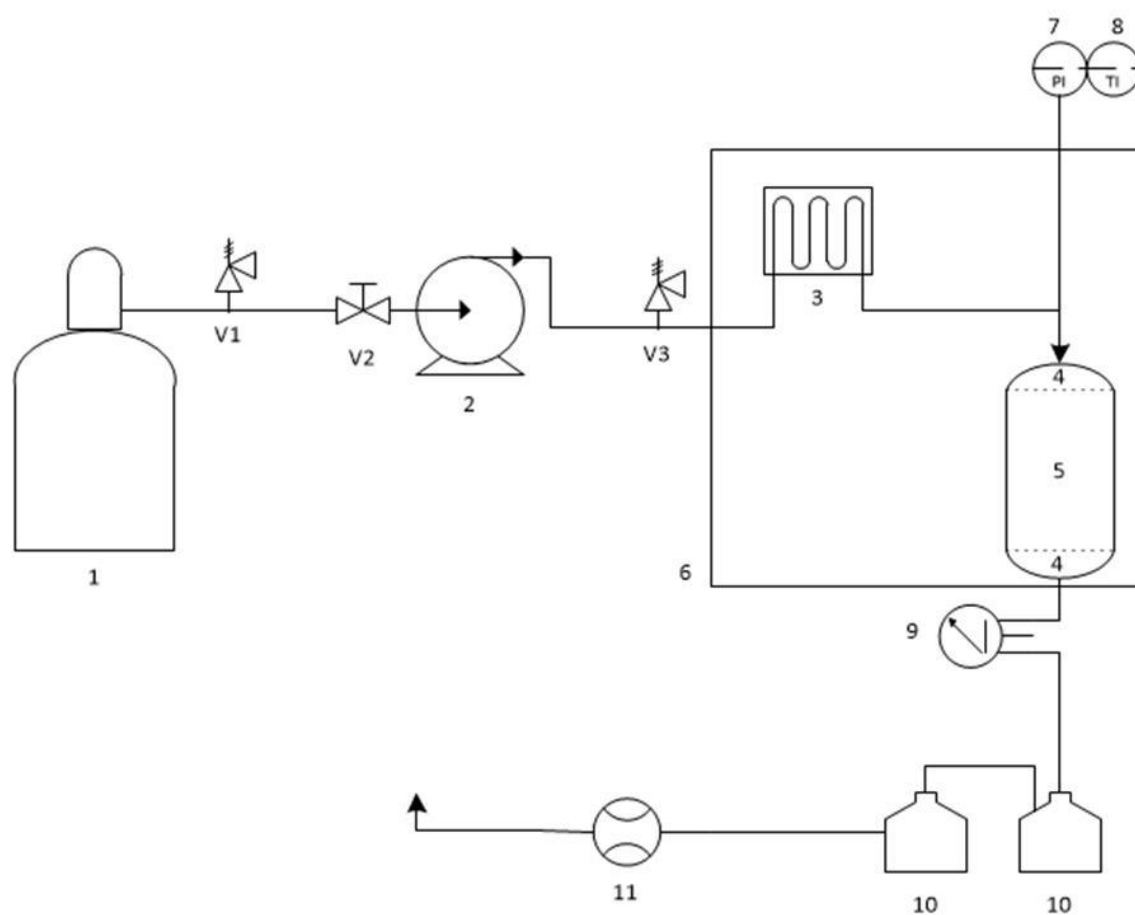
Tested model will be normally accepted if the percentage of average absolute relative deviation (AARD) is around 10% to 20% as this is the bench mark generally presented in literature [41–43]. However, in this study, the bench mark set was 10% and fitting of model to experimental data would only be shown if its AARD value was below 10%. A summary of constants in models and AARD of respective models to experimental values in subcritical and supercritical condition were shown in Table 5.

From Table 5, MST model correlates solubility data nicely in all conditions for both type of solute. The main difference between MST model and the other two is the consideration of solute vapor pressure factor in developing relation of solute solubility with density of solvent. Assumption in MST model is made that solute effect is negligible to density of solvent when solubility of solute is low [39]. Furthermore, as compared with Bartle and Chrastil model, MST model is a linear expression that does not include the reciprocal term of temperature [44]. The difference of deviation resulted between MST model and the other two models could possibly due to the assumption made and the linearity of the model. In MST model, two isotherms could collapse into a single line and this feature can be used to test the self-consistency of data and identify uncertain data points [35, 39, 45, 46]. This is because constants in MST model are independent of temperature, when data at different temperature are plotted, they will coincide into a single straight line. Correlations of suitable models with experimental data were illustrated through Figs. 6–9. In the diagram of showing comparison of model to experimental solubility data, datum points represented experimental data and solid line represented the data calculated by model.

From both Figs. 6 and 7, the MST model fitted the experimental data better in 302.15 K and lower density region in 298.15 K. At higher density region (600 – 800 kg/m³) in 298.15 K, the carbon dioxide density changed significantly with only 5 bar increment of pressure and making the carbon dioxide phase changed from gas to liquid. This sensitive behavior of carbon dioxide caused the MST model fits experimental solubility data less nicely to density of carbon dioxide in liquid phase. In addition, this could possibly because 302.15 K was near the critical temperature of carbon dioxide (304.25 K) and therefore these models that developed under supercritical background could fit nicer. From Fig. 8 and 9, MST semi-empirical model fitted experimental data better at lower temperature and this could because solute may experience some unpredictable phase changes at near melting point [6]. Although at ordinary condition melting points of camphene and caryophyllene oxide are higher, many unpredictable phase behavior change can be experience such as decline of solute melting point and inversion of density when solute is in contact with supercritical carbon dioxide [6].

5. Conclusions

Solubility of camphene and caryophyllene oxide in subcritical and supercritical carbon dioxide has been studied using dynamic method coupled with off-line analysis. This method had been prior validated with naphthalene. Solubility increases with increasing pressure at both subcritical and supercritical condition but influence of temperature on solubility is unpredictable because it depends on the dominancy effect which caused by retrograde behavior of solute-carbon dioxide system. When density effect of solvent dominates, lower solubility value is resulted at higher temperature. However, when solute sublimation pressure dominates, higher solubility value is resulted with higher temperature. Camphene and caryophyllene oxide have similar solubility behavior where their sublimation pressure dominates in subcritical condition and density effect dominates in supercritical condition. The similarity could possibly because they were both organic compound extracted from herb. Solubility of camphene and caryophyllene oxide was correlated nicely by Mendez-Santiago-Teja (MST) model by keeping the average absolute relative deviation (AARD) below 2%.



- | | |
|-------------------------------|----------------------------|
| 1: Carbon dioxide cylinder | 8: Temperature transmitter |
| 2: Positive displacement pump | 9: Back pressure regulator |
| 3: Preheating coil | 10: Solute trap |
| 4: Filters | 11: Dry gas meter |
| 5: Equilibrium cell | V1 and V3: Safety valve |
| 6: Oven | V2: Ball valve |
| 7: Pressure transmitter | |

Fig. 1. Experimental apparatus for measuring solubility.

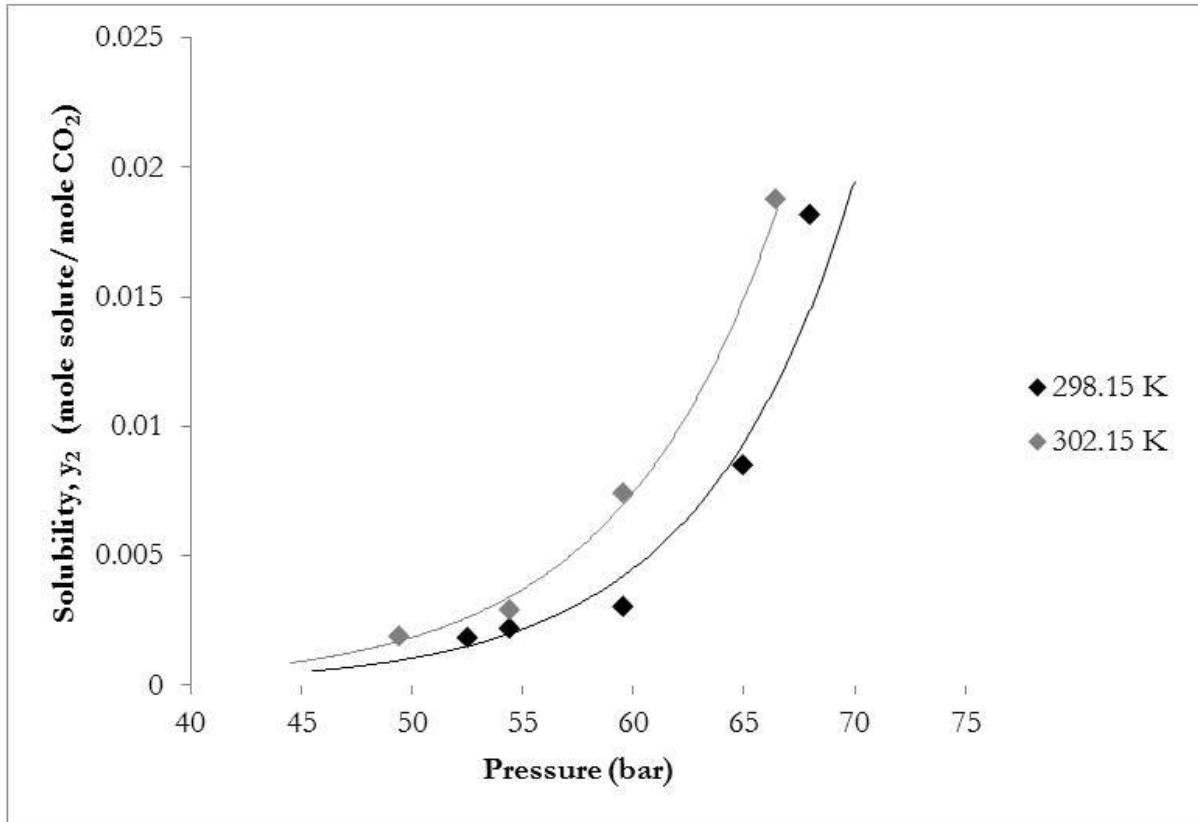


Fig. 2. Solubility of camphene in subcritical carbon dioxide.

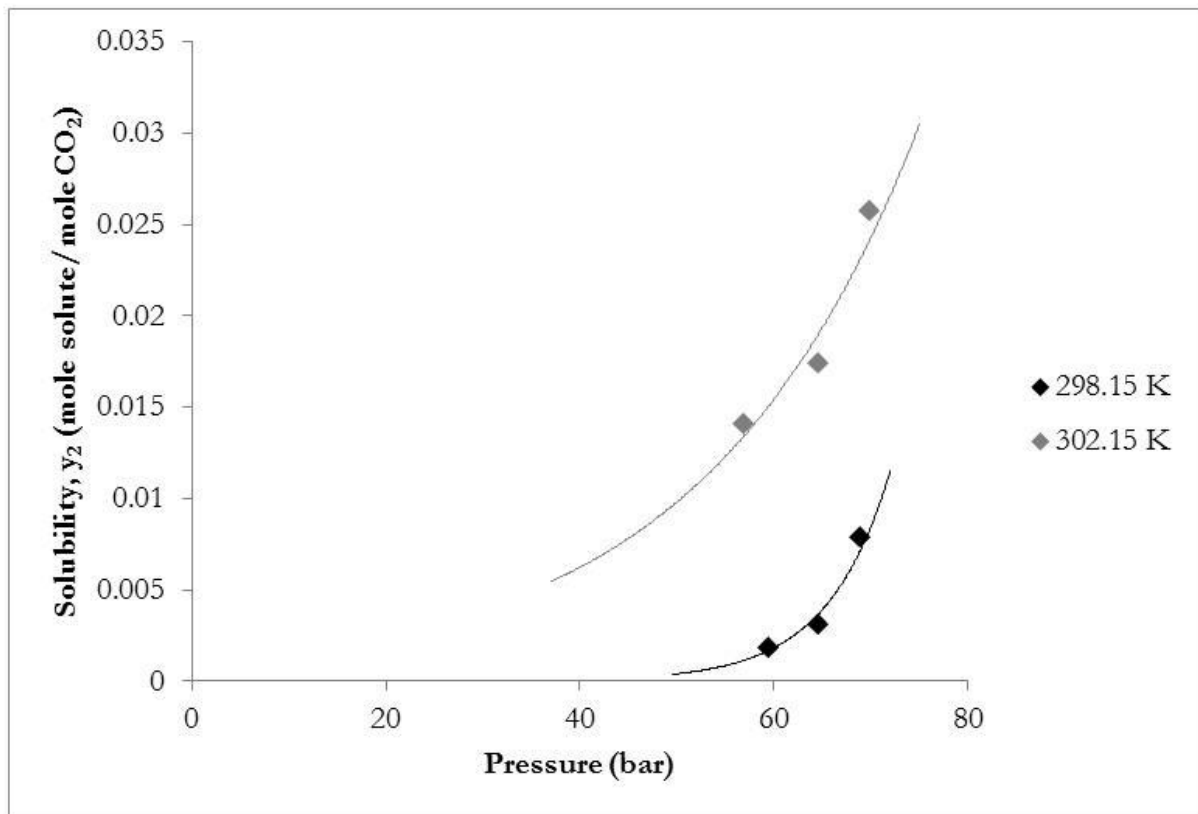


Fig. 3. Solubility of caryophyllene oxide in subcritical carbon dioxide.

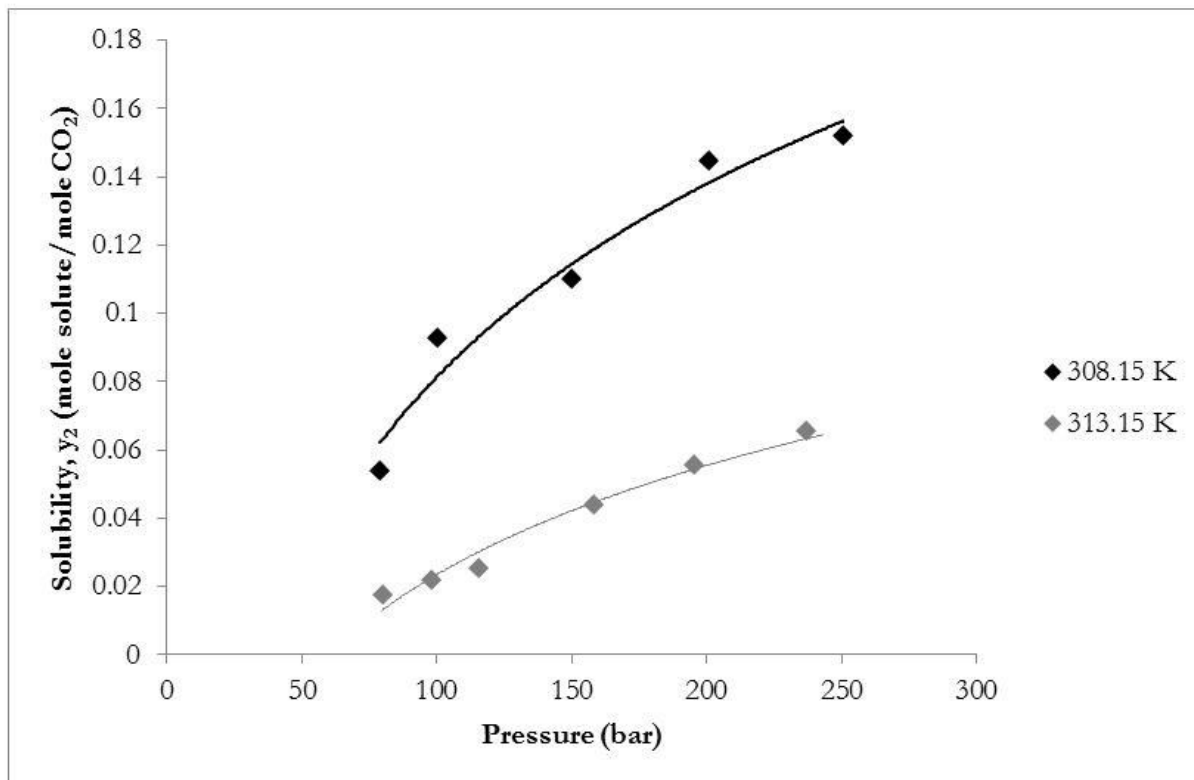


Fig. 4. Solubility of camphene in supercritical carbon dioxide.

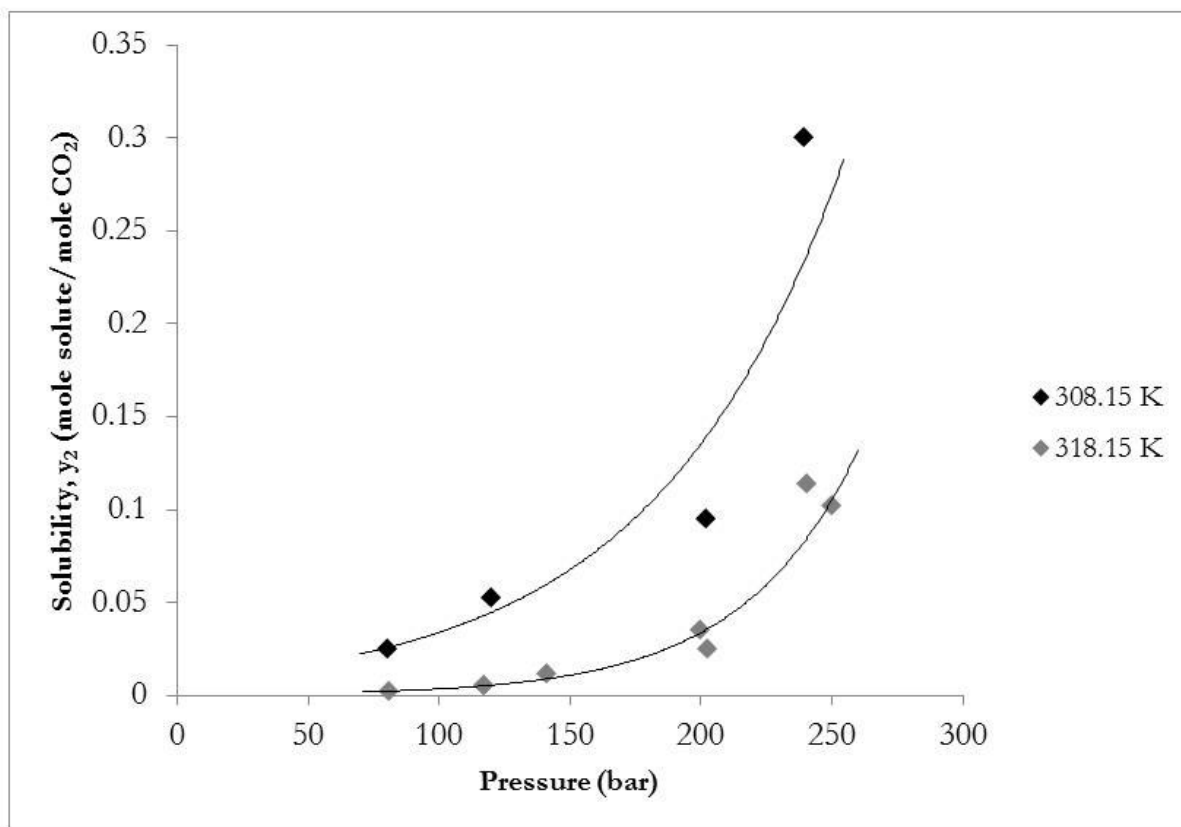


Fig. 5. Solubility of caryophyllene oxide in supercritical carbon dioxide.

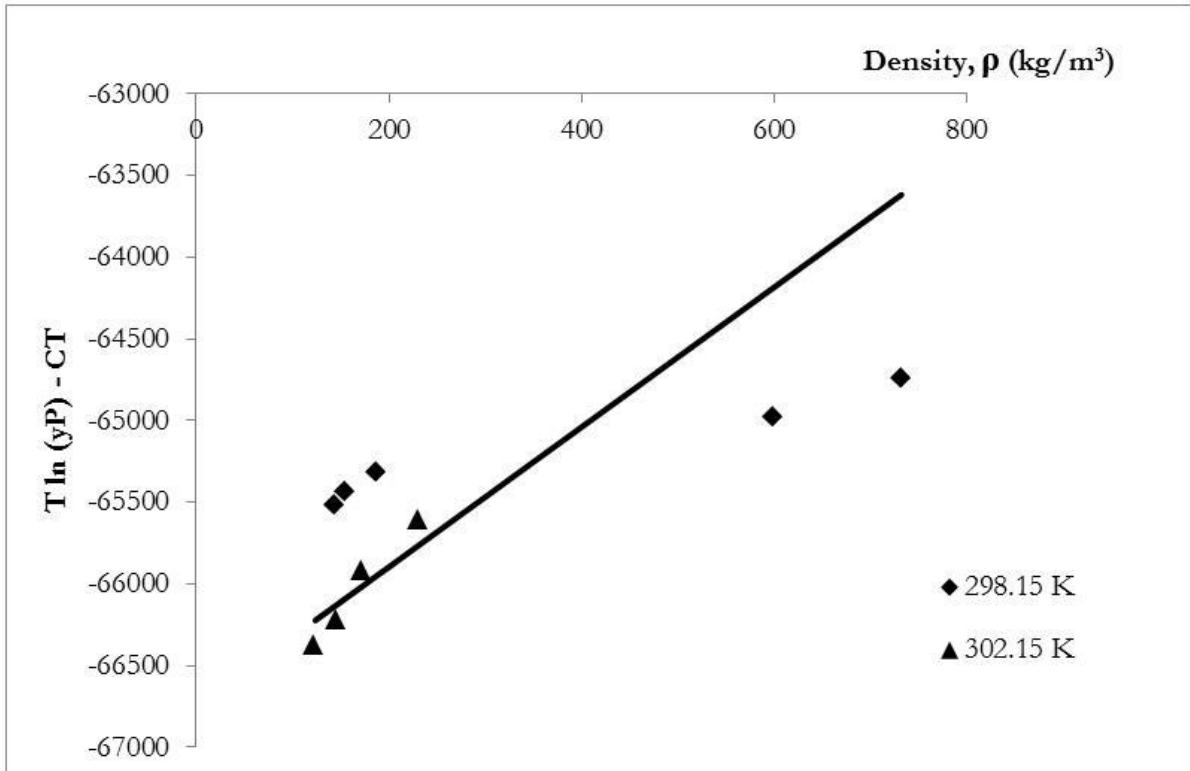


Fig. 6. Correlation of camphene subcritical solubility data by MST model.

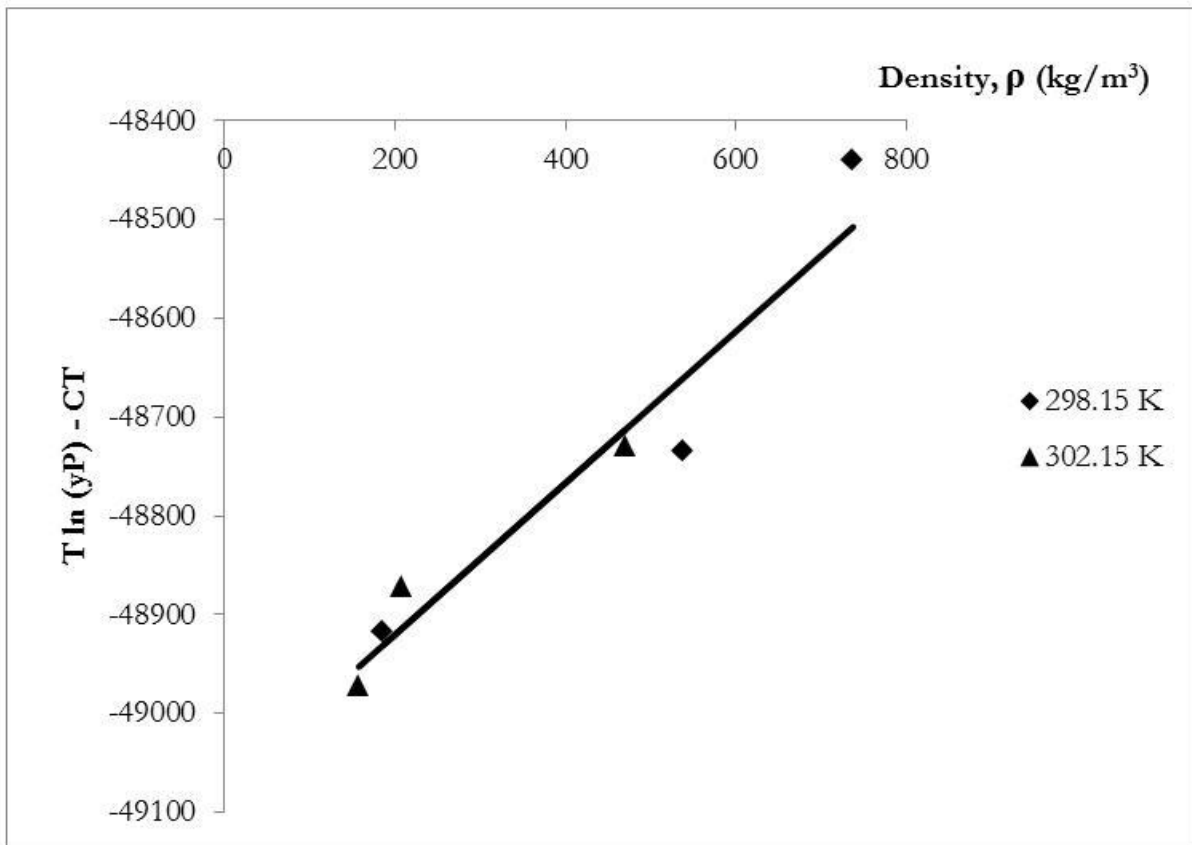


Fig. 7. Correlation of caryophyllene oxide subcritical solubility data by MST model.

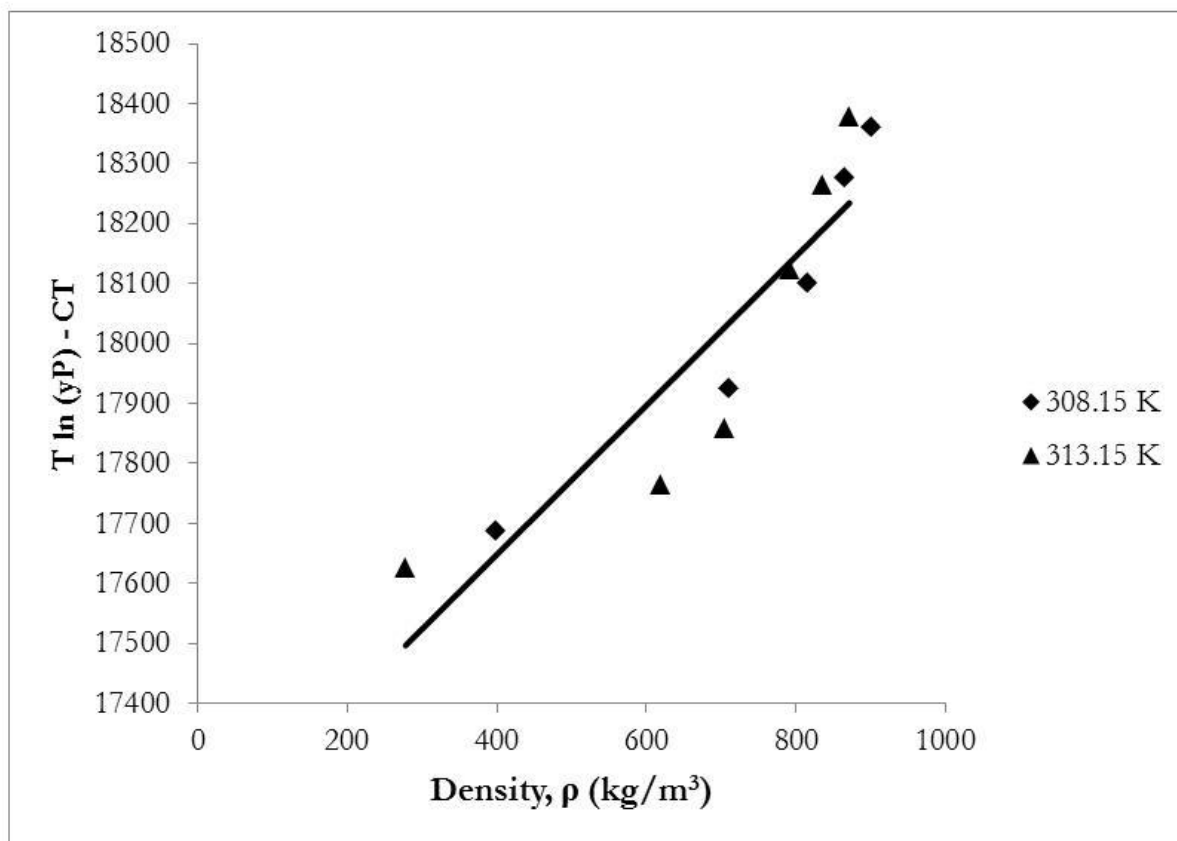


Fig. 8. Correlation of camphene supercritical solubility data by MST model.

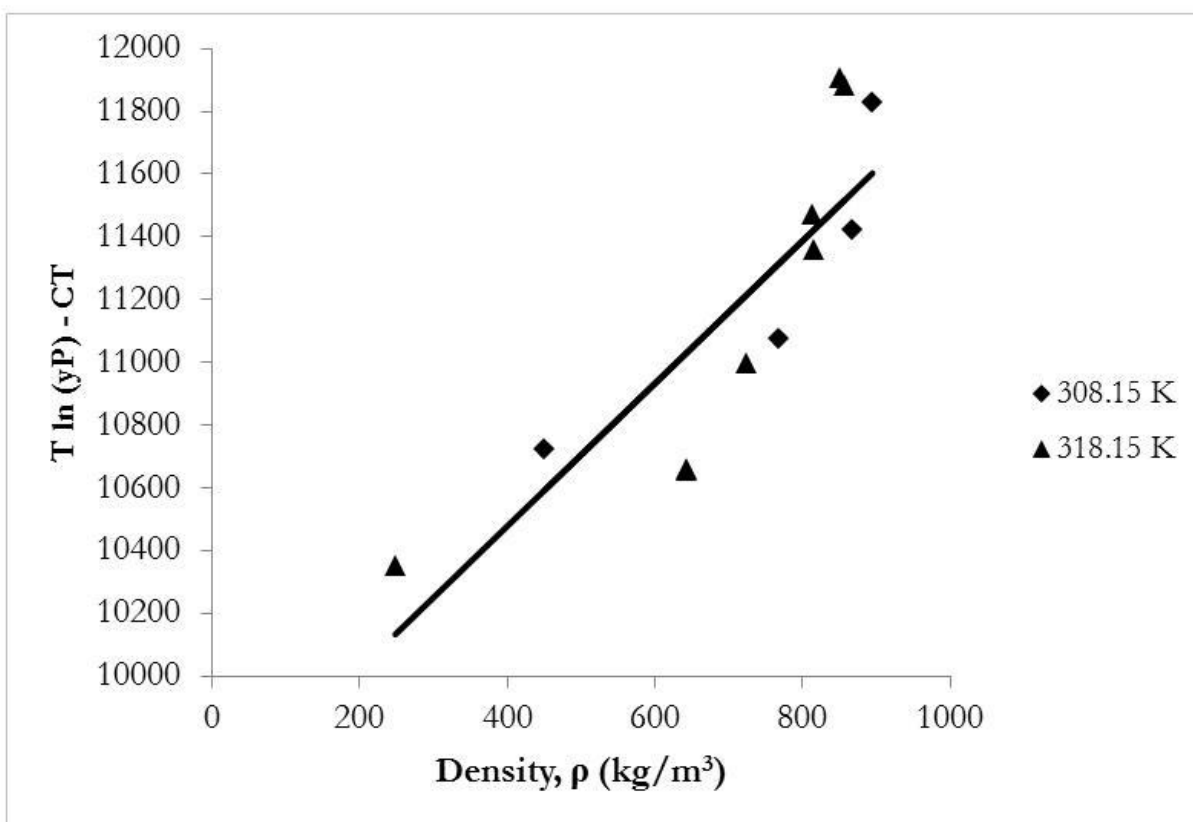


Fig. 9. Correlation of caryophyllene oxide supercritical solubility data by MST model.

Table 1. Experimental operating conditions.

Condition	Solute	Temperature (K)	Pressure (bar)
Subcritical	Camphene and caryophyllene oxide	298.15 and 303.15	50 – 70
Supercritical	Camphene	308.15 and 313.15	80 – 250
	Caryophyllene oxide	308.15 and 318.15	80 – 250

Table 2. Experimental solubility data of camphene.

Temperature (K)	Pressure (bar)	Gas mass (g)	Solute mass (g)	Solubility (mole fraction)
298.15	52.5	12.392	0.0667	1.738×10^{-3}
298.15	54.5	9.009	0.0600	2.151×10^{-3}
298.15	59.5	7.898	0.0733	2.999×10^{-3}
298.15	65.0	3.046	0.0800	8.483×10^{-3}
298.15	68.0	6.774	0.3800	1.812×10^{-2}
302.15	49.5	9.542	0.0567	1.918×10^{-3}
302.15	54.5	9.825	0.0867	2.849×10^{-3}
302.15	59.5	2.482	0.0567	7.374×10^{-3}
302.15	66.5	9.821	0.5704	1.876×10^{-2}
308.15	79.0	10.024	1.6767	5.402×10^{-2}
308.15	100.0	4.581	1.3133	9.260×10^{-2}
308.15	150.0	4.739	1.6133	1.100×10^{-1}
308.15	201.0	1.353	0.6054	1.445×10^{-1}
308.15	250.5	0.866	0.4067	1.517×10^{-1}
313.15	80.0	4.907	0.2667	1.755×10^{-2}
313.15	99.0	1.131	0.0767	2.189×10^{-2}
313.15	116.0	1.305	0.1033	2.558×10^{-2}
313.15	158.5	0.721	0.0967	4.330×10^{-2}
313.15	195.5	1.054	0.1800	5.516×10^{-2}
313.15	237.5	1.644	0.3333	6.549×10^{-2}

Table 3. Experimental solubility data of caryophyllene oxide.

Temperature (K)	Pressure (bar)	Gas mass (g)	Solute mass (g)	Solubility (mole fraction)
298.15	59.5	29.521	0.2667	1.840×10^{-3}
298.15	64.5	6.820	0.1067	3.123×10^{-3}
298.15	69.0	7.356	0.2900	7.872×10^{-3}
302.15	57.0	10.793	0.7567	1.400×10^{-2}
302.15	64.5	2.580	0.2233	1.729×10^{-2}
302.15	70.0	6.442	0.8267	2.562×10^{-2}
308.15	80.0	6.175	0.7700	2.490×10^{-2}
308.15	120.0	2.693	0.7067	5.240×10^{-2}
308.15	202.0	0.836	0.4000	9.554×10^{-2}
308.15	239.5	0.395	0.5933	2.999×10^{-1}
318.15	81.0	3.665	0.0467	2.543×10^{-3}
318.15	117.0	2.740	0.0633	4.692×10^{-3}
318.15	117.0	1.986	0.0467	4.616×10^{-3}
318.15	142.0	1.267	0.0700	1.103×10^{-2}
318.15	200.0	1.225	0.2133	3.477×10^{-2}
318.15	203.0	2.323	0.2833	2.435×10^{-2}
318.15	241.0	2.008	1.1400	1.134×10^{-1}
318.15	250.0	1.203	0.6167	1.024×10^{-1}

Table 4. Semi-empirical models used.

Semi-empirical model	Equation
Bartle	$\ln \frac{y_2 P}{P_{ref}} = \frac{A}{T} + B + C \rho_1$
Chrastil	$\ln c_2 = A + \frac{B}{T} + k \ln \rho_1$
Mendez-Santiago-Teja	$T \ln y_2 P - CT = A + B \rho_1$

y_2 is the solubility of solute (mole solute/mole CO₂), P is the system pressure (bar), P_{ref} is the reference pressure (1 bar), T is the system temperature (K), ρ_1 is the density of solvent (g/L or kg/m³), c_2 is the solubility of solute (g/L), k is the association number of solute, A , B and C are adjustable parameters.

Table 5. Mathematical modelling of solute solubility.

Condition	Solute	Model	A	B	C/k	AARD (%)
Subcritical	Camphene	Bartle	-65504	213.2	0.01425	293.49
		Chrastil	99.009	-35047	3.5253	419.92
		MST	-66753	4.2846	217.35	0.69
Subcritical	Caryophyllene oxide	Bartle	-48729	160.72	0.00255	36.27
		Chrastil	145.04	-45772	1.7362	8.19
		MST	-49074	0.7686	161.86	0.11
Supercritical	Camphene	Bartle	17986	-58.663	0.00405	27.31
		Chrastil	-71.323	19388	2.1074	4.18
		MST	17151	1.2435	-55.944	0.51
Supercritical	Caryophyllene oxide	Bartle	11198	-39.333	0.0073	58.72
		Chrastil	-60.321	12896	3.66535	17.11
		MST	9567.8	2.2759	-34.108	1.95

References

- [1] Q. S. Li, Z. T. Zhang, C. L. Zhong, Y. C. Liu, and Q. R. Zhou, "Solubility of solid solutes in supercritical carbon dioxide with and without cosolvents," *Fluid Phase Equilibria*, vol. 207, pp. 183–192, 2003.
- [2] K. Grodowska and A. Parczewski, "Organic Solvents in the Pharmaceutical Industry," *Acta Poloniae Pharmaceutica - Drug Research*, vol. 67, no. 1, pp. 3–12, 2010.
- [3] E. J. Beckman, "Supercritical and near-critical CO₂ in green chemical synthesis and processing," *Journal of Supercritical Fluids*, vol. 28, pp. 121–191, 2004.
- [4] D. L. Reger, S. R. Goode, and D. W. Ball, "Liquids and solids," in *Chemistry: Principles and Practices Canada*. Canada: Cengage Learning, 2009, ch. 11, pp.436.
- [5] G. Subramanian, *Process Scale Liquid Chromatography*. Weinheim: John Wiley and Sons, 2008, pp. 165.
- [6] A. M. A. Karim, D. M. Kassim, and M. S. Hameed, "Phase equilibrium study for the separation of solid components using supercritical carbon dioxide," *The Open Thermodynamics Journal*, vol. 4, pp. 201–211, 2010.
- [7] S. N. Reddy and G. Madras, "Solubilities of benzene derivatives in supercritical carbon dioxide," *Journal of Chemical and Engineering Data*, vol. 56, pp. 1695-1699, 2011.
- [8] World Health Organization, "IARC Monographs on the evaluation of carcinogenic risks to humans," in *IARC. Betel-Quid and Areca-Nut Chewing and Some Areca-Nut-Derived Nitrosamines*. Lyon: IARC Press, 2004, vol. 85, pp. 33–34.
- [9] R. K. Chalannavar, V. K. Narayanaswamy, H. Baijnath, and B. Odhav, "Chemical composition of essential oil of Psidium cattleianum var. lucidum (Myrtaceae)," *African Journal of Biotechnology*, vol. 11, no. 33, pp. 8341–8347, 2012.
- [10] M. J. Chavan, P. S. Wakte, and D. B. Shinde, "Analgesic and anti-inflammatory activity of Caryophyllene oxide from Annona squamosa L. bark," *Phytomedicine*, vol. 17, pp. 149–151, 2010.

- [11] A. Kadri, N. Gharsallah, M. Damak, and R. Gdoura, "Chemical composition and in vitro antioxidant properties of essential oil of *Ricinus communis* L.," *Journal of Medicinal Plants Research*, vol. 5, no. 8, pp. 1466–1470, 2011.
- [12] H. Amiri, "Antioxidant activity of the essential oil and methanolic extract of *Teucrium orientale* (L.) subsp. *taylori* (Boiss.) Rech. f.," *Iranian Journal of Pharmaceutical Research*, vol. 9, no. 4, pp. 417–423, 2010.
- [13] J. F. Li, N. Liang, Z. Sun, R. J. Du, B. Shi, and X. H. Hou, "Simultaneous determination of isoquinoline, caryophyllene oxide, hexadecane in essential oils from *Juglandis Mandshuricae* Cortex by vapour-vapour extraction combined with gas chromatograph analysis," *Asian Journal of Traditional Medicines*, vol. 7, no. 6, pp. 246–252, 2012.
- [14] M. A. Hossain, Z. Ismail, A. Rahman, and S. C. Kang, "Chemical composition and anti-fungal properties of the essential oils and crude extracts of *Orthosiphon stamineus* Benth.," *Industrial Crops and Products*, vol. 27, pp. 328–334, 2008.
- [15] B. M. Hybertson, "Solubility of the sesquiterpene alcohol patchoulol in supercritical carbon dioxide." *Journal of Chemical and Engineering Data*, vol. 52, no. 1, pp. 235–238, 2007.
- [16] P. F. de Oliveira, R. A. F. Machado, A. Bolzan, and D. Barth, "Supercritical fluid extraction of hernandulcin from *Lippia dulcis* Trev.," *Journal of Supercritical Fluids*, vol. 63, pp. 161–168, 2012.
- [17] C. Garlapati and G. Madras, "Solubilities of dodecanoic and tetradecanoic acids in supercritical CO₂ with and without entrainers," *Journal of Chemical and Engineering Data*, vol. 53, pp. 2637–2641, 2008.
- [18] H. B. Xing, Y. W. Yang, B. G. Su, M. Huang, and Q. L. Ren, "Solubility of artemisinin in supercritical carbon dioxide," *Journal of Chemical and Engineering Data*, vol. 48, pp. 330–332, 2003.
- [19] W. C. Tsai, Y. H. Ruan, and S. S. H. Rizvi, "Solubility measurement of methyl anthranilate in supercritical carbon dioxide using dynamic and static equilibrium systems," *Journal of the Science of Food and Agriculture*, vol. 86, pp. 2083–2091, 2006.
- [20] A. C. Kumoro, "Solubility of corosolic acid in supercritical carbon dioxide and its representation using density-based correlations," *Journal of Chemical and Engineering Data*, vol. 56, pp. 2181–2186, 2011.
- [21] R. L. Mendes, B. P. Nobre, J. P. Coelho, and A. F. Palavra, "Solubility of β -carotene in supercritical carbon dioxide and ethane," *Journal of Supercritical Fluids*, vol. 16, pp. 99–106, 1999.
- [22] C. S. Su and Y. P. Chen, "Correlation for the solubilities of pharmaceutical compounds in supercritical carbon dioxide," *Fluid Phase Equilibria*, vol. 254, pp. 167–173, 2007.
- [23] H. Perrotin-Brunel, M. C. Kroon, M. J. E. van Roosmalen, J. van Spronsen, C. J. Peters, and G. J. Witkamp, "Solubility of non-psychoactive cannabinoids in supercritical carbon dioxide and comparison with psychoactive cannabinoids," *Journal of Supercritical Fluids*, vol. 55, pp. 603–608, 2010.
- [24] H. S. Yeoh, G. H. Chong, N. Mohd Adzahan, R. Abdul Rahman, and T. S. Y. Choong, "Solubility measurement method and mathematical modeling in supercritical fluids," *Engineering Journal*, vol. 17, no. 3, pp. 67–78, 2013.
- [25] M. McHugh and M. E. Paulaitis, "Solid solubilities of naphthalene and biphenyl in supercritical carbon dioxide," *Journal of Chemical Engineering Data*, vol. 25, pp. 326–329, 1980.
- [26] G. T. Liu and K. Nagahama, "Solubility of organic solid mixture in supercritical fluids," *Journal of Supercritical Fluids*, vol. 9, pp. 152–160, 1996.
- [27] A. Dams and E. U. Schlunder, "Mass transfer in supercritical fluid extraction of a binary aromatic mixture, naphthalene and phenanthrene, from porous rods," *Chemical Engineering and Processing: Process Intensification*, vol. 30, no. 2, pp. 69–78, 1991.
- [28] A. Akgerman and M. Girdhar, "Fundamentals of solids extraction by supercritical fluids," in *Supercritical Fluids - Fundamentals for Applications*. Netherlands: Kluwer Academic Publishers, 1994, pp. 669.
- [29] C. E. Ophardt. (2003). *Temperature and Pressure Effects on Solubility*. Virtual Chembook. Available: <http://www.elmhurst.edu/~chm/vchembook/174tempres.html>
- [30] J. M. Aguilera, R. Simpson, J. Welti-Chanes, D. B. Aguirre, and G. Barbosa-Canovas, *Food Engineering Interfaces*. New York: Springer, 2010, pp. 359.
- [31] K. K. Liang, N. R. Foster, and S. S. T. Ting, "Solubility of fatty acid esters in supercritical carbon dioxide," *Industrial and Engineering Chemistry Research*, vol. 31, pp. 400–404, 1992.
- [32] G. G. Simeoni, T. Bryk, F. A. Gorelli, M. Krisch, G. Ruocco, M. Santoro, and T. Scopigno, "The Widom line as the crossover between liquid-like and gas-like behaviour in supercritical fluids," *Nature Physics*, vol. 6, pp. 503–507, 2010.

- [33] K. Jinno, H. Nagashima, K. Itoh, M. Saito, and M. Buonoshita, "Subcritical fluid extraction and supercritical fluid chromatography of carbon clusters C60 and C70," *Fresenius Journal of Analytical Chemistry*, vol. 344, pp. 435–441, 1992.
- [34] S. Otles. (2005). *Supercritical Fluid Extraction* [Online]. Available: <http://eng.ege.edu.tr/~otles/SupercriticalFluidsScienceAndTechnology/Wc96f5b3b43272.htm>
- [35] A. Z. Hezave, A. Mowla, and F. Esmailzadeh, "Cetirizine solubility in supercritical carbon dioxide at different pressures and temperatures". *Journal of Supercritical Fluids*, vol. 58, pp. 198–203, 2011.
- [36] S. A. Shojaee, H. Rajaei, A. Z. Hezave, M. Lashkarbolooki, and F. Esmailzadeh, "Experimental measurement and correlation for solubility of piroxicam (a non-steroidal anti-inflammatory drugs (NSAIDs)) in supercritical carbon dioxide," *Journal of Supercritical Fluids*, vol. 80, pp. 38–43, 2013.
- [37] K. D. Bartle, A. A. Clifford, S. A. Jafar, and G. F. Shilstone, "Solubilities of solids and liquids of low volatility in supercritical carbon dioxide," *Journal of Physical and Chemical Reference Data*, vol. 20, pp. 713–756, 1991.
- [38] J. Chrastil, "Solubility of solids and liquids in supercritical gases," *The Journal of Physical Chemistry*, vol. 86, pp. 3016–3021, 1982.
- [39] J. Mendez-Santiago and A. S. Teja, "The solubility of solids in supercritical fluids," *Fluid Phase Equilibria*, vol. 158–160, pp. 501–510, 1999.
- [40] R. B. Gupta and J. J. Shim, *Solubility in Supercritical Carbon Dioxide*. United States: CRC Press, 2007.
- [41] M. A. Sabegh, H. Rajaei, F. Esmailzadeh, and M. Lashkarbolooki, "Solubility of ketoprofen in supercritical carbon dioxide," *Journal of Supercritical Fluids*, vol. 72, pp. 191–197, 2012.
- [42] K. Khimeche, P. Alessi, I. Kikic, and A. Dahmani, "Solubility of diamines in supercritical carbon dioxide: Experimental determination and correlation," *Journal of Supercritical Fluids*, vol. 41, pp. 10–19, 2007.
- [43] M. H. Hosseini, N. Alizadeh, and A. R. Khanchi, "Solubility analysis of clozapine and lamotrigine in supercritical carbon dioxide using static system," *Journal of Supercritical Fluids*, vol. 52, pp. 30–35, 2010.
- [44] P. Coimbra, M. R. Blanco, H. S. R. Costa Silva, M. H. Gil, and H. C de Sousa, "Experimental determination and correlation of Artemisinin's solubility in supercritical carbon dioxide," *Journal of Chemical and Engineering Data*, vol. 51, pp. 1097–1104, 2006.
- [45] M. Mirzajanzadeh, F. Zabihi, and M. Ardjmand, "Measurement and correlation of Ibuprofen in supercritical carbon dioxide using Stryjek and Vera EOS," *Iranian Journal of Chemical Engineering*, vol. 7, no. 4, pp. 42–49, 2010.
- [46] G. H. Tian, J. S. Jin, Z. T. Zhang, and J. J. Guo, "Solubility of mixed solids in supercritical carbon dioxide," *Fluid Phase Equilibria*, vol. 251, pp. 47–51, 2007.